Computational investigation of Tb(III) ion line intensities in single-bubble sonoluminescence

Jinfu Liang[1,2,3] and Yu An[1,*]

[1]*Department of Physics, Tsinghua University, Beijing 100084, China*

[2]*School of Physics and Electronic Science, Guizhou Normal University, Guiyang 550001, China*

[3]*Guizhou Provincial Key Laboratory of Radio Astronomy and Data Processing, Guizhou Normal University, Guiyang 550001, PR China*

(Received 15 July 2017; revised manuscript received 24 September 2017; published 28 December 2017)

We perform a computational fluid dynamics simulation of trivalent terbium [Tb(III)] ion line emissions from single-bubble sonoluminescence (SBSL). Our simulation includes dynamic boundary conditions as well as the effects of gas properties and quenching by species, such as nitrite ion (NO_2^-). Simulation results demonstrate that when the maximum temperature inside a dimly luminescing bubble is relatively low, emission peaks from excited Tb(III) ions are prominent within the emission spectra. As the maximum temperature of the bubble increases, emission peaks of Tb(III) ions fade away relative to the continuum background emission. These calculations match observations of Tb(III) line emissions from SBSL occurring in aqueous solutions of terbium nitrate [$Tb(NO_3)_3$] under an argon gas atmosphere. The evolution of the radiation energy spectrum over time for sonoluminescing bubbles provides a clear mechanism explaining Tb(III) emission peaks gradually merging into the continuous background emission as the radiation power increases.

DOI: 10.1103/PhysRevE.96.063118

I. INTRODUCTION

Single-bubble sonoluminescence (SBSL) describes the phenomenon of light emitted during the implosive collapse of a single isolation gas bubble driven by a strong ultrasound wave. SBSL was first observed by Gaitan *et al.* in 1992 [1]. The gas bubble can oscillate for hours near an antinode of a standing acoustic field, emitting a picosecond-long burst of light once every acoustic cycle [2]. Light emission results, in part, from the excitation of ion species within the bubble caused by an extreme increase in temperature and pressure while the bubble collapses. An explantation of the mechanism behind the line emission from nonvolatile species injecting into a bubble from the host liquid is proposed here.

Until now, SBSL has been studied theoretically [3–7] and experimentally [8–11]. Two models have been proposed to explain how nonvolatile species are heated in a collapsing bubble: the shell model and the injected droplet model [4]. According to the shell model, nonvolatile metal ions at the gas-liquid interface at the bubbles' edges are reduced and excited by radicals formed within the gas. According to the injected droplet, nanodroplets of liquid are nebulized into the bubble by capillary surface waves resulting from instabilities at the gas-liquid interface. Nonvolatile metal ions carried by these nanodroplets then are excited due to the extreme temperatures achieved by the core of the bubble during collapse. Directly experimental evidence in favor of either model has been difficult to obtain because SBSL occurs very quickly in small volumes. Each model has theoretical drawbacks. Theoretical calculations also suggest that the interfacial region between the liquid and the gas inside the bubble may not reach the temperatures required by the shell model [12]. For the injected droplet model, the processes of vapor supersaturation and microjetting during collapse are not fully understood [13].

In 1999, Hilgenfeldt *et al.* proposed a simple model to interpret the experimental data available for SBSL quantitatively, according to which the temperature and pressure inside the bubble were assumed to be uniform and vapor effects were neglected [3]. In 2008, An *et al.* improved upon this analysis by using numerical calculations utilizing computational fluid dynamics (CFD) simulations that include appropriate moving boundary conditions and vapor effects. Their calculations suggest a possible mechanism for how the Na emission peak near 589 nm and the OH emission peak near 310 nm merge into the continuum background emission as the total radiation power increases [6,7]. Their numerical simulation also showed that spectral lines are prominent when the maximum temperature inside a dimly luminescing bubble remains relatively low. As the maximum temperature at the core of the bubble increases in their simulation, the line emission peaks weaken and fade into the continuum background [7]. These simulations show that the temperature inside a sonoluminescing bubble may be inferred from observations of line spectra.

Recently, considering lanthanide ions as optical emissive probes for SL, several groups have studied experimentally lanthanide ions excited by strong ultrasound in aqueous solution. In 2010, Sharipov *et al.* detected spectral lines of Tb(III), trivalent cesium ions [Ce(III)], and trivalent praseodymium [Pr(III)] emitted via SBSL. Their experimental results indicated a low probability of nonvolatile metal ions penetrating into the center of the bubble, which weighs in favor of the injected-droplet model [14]. In 2013, Pflieger *et al.* studied SBSL in a Tb(III) solution excited using ultrasound at several frequencies [15]. Our laboratory also has observed Tb(III) spectral lines in the emission from Ar bubbles generated in an aqueous solution constituting terbium chloride ($TbCl_3$) or terbium nitrate [$Tb(NO_3)_3$] under a 100 Torr Ar atmosphere [16], which shows that Tb(III) ion is a good green-light emitter with more energy level structures. It is of interest to explore the mechanism behind Tb(III) emission during SL.

We reproduce those experimental results in Fig. 1 for easy reference. The intensities of Tb(III) line emissions increase with increasing amplitude of driving sound pressure (p_a). The spectral lines result from the transition of Tb(III) from its

*Corresponding author: anyuw@mail.tsinghua.edu.cn

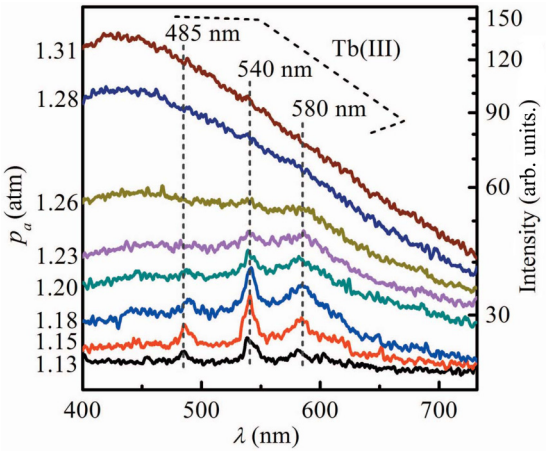

FIG. 1. SBSL spectra from $Tb(NO_3)_3$ aqueous solutions under 100 Torr of argon (Ar) gas. The vertical dashed lines show three central wavelengths of spectral peaks.

first excited state ($^5D_4$) to its ground state ($^7F_{J\,(J=6,5,4,\ldots,0)}$) [17]. The spectral peaks around 485, 540, and 580 nm in Fig. 1 correspond to the $^5D_4 \rightarrow {}^7F_6$, $^5D_4 \rightarrow {}^7F_5$, and $^5D_4 \rightarrow {}^7F_4$ transitions, respectively.

While p_a is relatively low, emission lines from Tb(III) are prominent within the emission spectrum. As p_a increases, the spectral peaks gradually fade into the background continuum. The mechanism behind this observed variation of the Tb(III) spectral peaks with p_a remained unclear in our previous report. Herein, we employ the model reported in Refs. [5–7] to simulate the spectral lines emitted from Tb(III) ions during SBSL and illuminate the mechanism behind their emission.

II. THEORETICAL MODEL

The theoretical model employed herein is similar to that reported in Refs. [5–7]. In this model, fluid mechanics equations for two main kinds of gas components, Ar and water vapor, describe the gas dynamics inside the bubble. Since evaporation and condensation of water vapor occur at the bubble wall, the law of mass action is applied to evaluate the products of the ionization reaction, considering phase of transitions and heat exchange at the bubble wall. The emission spectra of Tb(III) ions (around 485, 540, 580, 615, 645, 670, and 680 nm), the radiative attachment of electrons to atoms or molecules, and bremsstrahlung (electron-neutral atom and electron-ion) and recombination radiations all are accounted for in our model. The boundary at the moving bubble wall is described by the Rayleigh-Plesset (RP) equation.

For the RP equation governing the variation of the bubble radius, we adopt the following form [18]:

$$(1-M)R\ddot{R}+\frac{3}{2}\left(1-\frac{M}{3}\right)\dot{R}^2 = (1+M)\frac{1}{\rho_l}[p_l-p_\infty-p_s(t+t_R)]+\frac{t_R}{\rho_l}\dot{p}_l, \quad (1)$$

where t is the time, $R(t)$ is the radius of the bubble, p_∞ is the ambient pressure, $p_s(t)=-P_a\sin(\omega t)$ is the driving acoustic pressure, and p_a is the amplitude of sound pressure. ω is the frequency of the acoustic wave, $t_R=\frac{R}{c_l}$, and c_l and ρ_l are the sound speed and the liquid density on the liquid side of the bubble wall, respectively. $p_l=p_g(R,t)-4\mu\frac{\dot{R}}{R}-\frac{2\sigma}{R}$ is the pressure on the liquid side of the surface wall, μ is the dynamic viscosity, and σ is the surface tension coefficient for the liquid. $M\equiv\frac{\dot{R}}{c_l}$ is the bubble-wall Mach number, which represents effects due to the compressibility of the liquid.

The function for radiation power is taken from Ref. [5],

$$P(\lambda,t)=8\pi^2\int_0^R\int_{-1}^1 k_\lambda(r)P_\lambda^{pI}(r) \times\exp\left(-\int_{rx}^{\sqrt{R^2-r^2(1-x^2)}}k_\lambda ds\right)r^2dr\,dx, \quad (2)$$

which describes the total power emitted from the bubble for each acoustic cycle at wavelength λ. In this equation, r is the radial distance from the center of the bubble. P_λ^{PI} is the Planck radiation intensity, and k_λ is the absorption coefficient.

For the line emission spectra,

$$k_\lambda=\frac{\lambda^5}{2hc^2}(e^{hc/\lambda kT}-1)P_\lambda, \quad (3)$$

where P_λ represents the radiation power per unit volume per unit wavelength interval of the line spectrum. Herein, we mainly consider the $^5D_4 \rightarrow {}^7F_J$ ($J=6,5,4,\ldots,0$) transitions of Tb(III).

For line emissions from Tb(III), we suppose that thermal excitation dominates the formation of excited Tb(III) ions during SBSL. For the $i \rightarrow j$ transition, the radiation power per unit volume may be calculated as

$$P_{i,j}=\frac{fn_ag_ie^{-(E_i/kT)}}{\sum g_i/kT}A_{i,j}h\nu_{i,j}, \quad (4)$$

where f is a factor to estimate the quenching of the radiation by collisions with other particles [23], such as NO_2^{-1}, n_a is the number density of Tb(III) ions inside the bubble, $A_{i,j}$ is the transition probability [24,25], $h\nu_{i,j}$ is the photon energy, and g_i is the Landé factor of the ith energy level E_i.

The distribution of the intensities of line spectra emitted by SBSL is assumed to be even. The radiation power from Tb(III) radicals per unit volume per wavelength interval is given by

$$P_\lambda d\lambda=P_{i,j}g_{i,j}\left(\nu=\frac{c}{\lambda}\right)\frac{c}{\lambda^2}d\lambda, \quad (5)$$

where ν is the emission frequency and $g_{i,j}$ is the following Lorentzian function:

$$g_{i,j}(\nu)=\pi\frac{\Delta\nu/2}{(\nu-\nu_{i,j})^2+(\Delta\nu/2)^2}. \quad (6)$$

For collision and resonance broadening [19],

$$\Delta\nu=\sigma_0\nu_0n/\pi+50\frac{n_af_a}{\nu_{i,j}}, \quad (7)$$

where σ_0 is the collision cross section, ν_0 is the average relative speed of molecules in the gas, n is the number of particles present, and f_a is the absorption oscillator strength. We determine the cross sections for collisions from the diameters of the gas molecules.

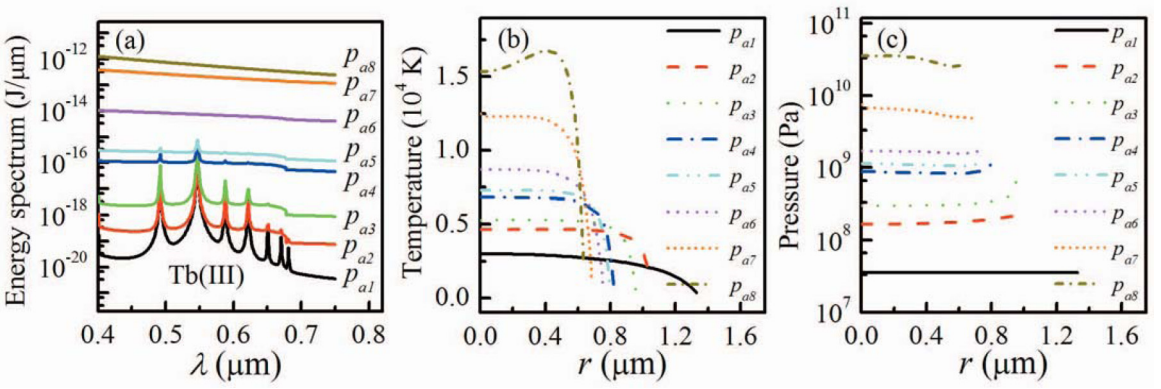

FIG. 2. An Ar bubble in $Tb(NO_3)_3$ aqueous solutions at 15 °C driven at eight different pressures, $p_a = 1.13$, 1.15, 1.18, 1.20, 1.23, 1.26, 1.28, and 1.31 atm are labeled as p_{ai} ($i = 1,2,...,8$, respectively). (a) Energy spectra, (b) temperature when the bubble reaches its minimum size, and (c) corresponding pressure.

The total radiation power is the integral over the relevant wavelengths λ,

$$P(t) = \int_{400\,\mathrm{nm}}^{750\,\mathrm{nm}} P(\lambda,t)d\lambda. \tag{8}$$

We also can evaluate the cumulative radiation energy emitted from a SBSL bubble over the time 0 to t within each acoustic period,

$$E_\lambda(t) = \int_0^t P(\lambda,t')dt', \quad 0 \leqslant t \leqslant \frac{2\pi}{\omega}. \tag{9}$$

Since SBSL occurs for only a few hundred picoseconds in each acoustic cycle, only during that short duration does $P(\lambda,t)$ not vanish.

III. RESULTS AND DISCUSSION

A. Spectral characteristics of Tb(III) emission

Below, we calculate Tb(III) line emission peaks that stand out from continuum background emissions. Based on our experimental data, we consider a bubble containing Ar gas of ambient radius $R_0 = 4.80$ μm in a 15 °C aqueous solution of $Tb(NO_3)_3$ driven with an acoustic wave of frequency 25.80 kHz. To obtain an approximate quantitative prediction of the Tb(III) peaks in the SBSL emission spectrum, we assume that the Tb(III) line originates from thermally excited Tb(III) ions within the gas bubble and set the number density of Tb(III) particles n_a in Eq. (4) as $n \times 10^{-5}$ (n is the total number density of particles inside the bubble). We simulate the Ar bubble in a 15 °C aqueous solution of $Tb(NO_3)_3$ for eight values of driving pressure ($p_{a1}, p_{a2}, \ldots, p_{a8}$) in Fig. 2.

For the sake of simplicity, we treat the aqueous solution of $Tb(NO_3)_3$ as if it were simply water in our calculation. The Tb(III) spectral lines in the regions of 0.48–0.69 μm are distinct at the lowest amplitude of driving acoustic pressure $p_a = 1.13$ atm. As p_a increases, the total emission intensity of SBSL increases, and the Tb(III) spectral lines gradually disappear.

Although an exact comparison between the simulation results and the observed data is impossible, the simulation results follow a similar trend as that of the experimental data presented in Fig. 1, insofar as the Tb(III) line emissions fade relative to the continuum background with increasing radiation intensity. We therefore judge that our CFD simulation models the SBSL system reasonably well. Figures 2(b) and 2(c) plot simulated distributions of temperature and pressure inside the bubble at its minimum radius.

While the core temperature remains below about 8200 K (corresponding to a pressure of about 1.90×10^9 Pa), the Tb(III) emission peaks stand out from the continuum background. As the temperature rises, the Tb(III) emission peaks fade away into the continuum background. To illustrate this trend, we introduced a quantity (β) to describe the contrast of the spectral line and its continuum background [20], that is

$$\beta = \frac{I_{\mathrm{line}} - I_{\mathrm{bg}}}{I_{\mathrm{bg}}}, \tag{10}$$

where I_{line} and I_{bg} are the intensities of the most prominent spectral line and its continuum background, respectively.

Figure 3 shows the trend that β decreases with the increase in the maximum temperature inside a bubble, which means the emission of light contributed to the Tb(III) line decreases with increasing bubble luminance. These findings reveal that sonoluminescent bubbles reaching different maximum temperatures should present different spectral emission profiles.

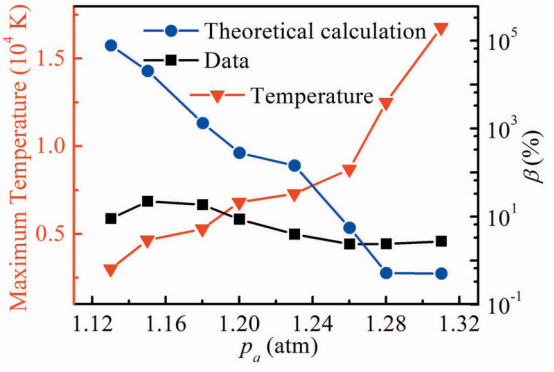

FIG. 3. Calculation of maximum temperature and β versus the amplitude of acoustic pressure (p_a), respectively. We only select the intensity of spectral line at $\lambda = 540$ nm and its continuum background obtained by the interpolation method.

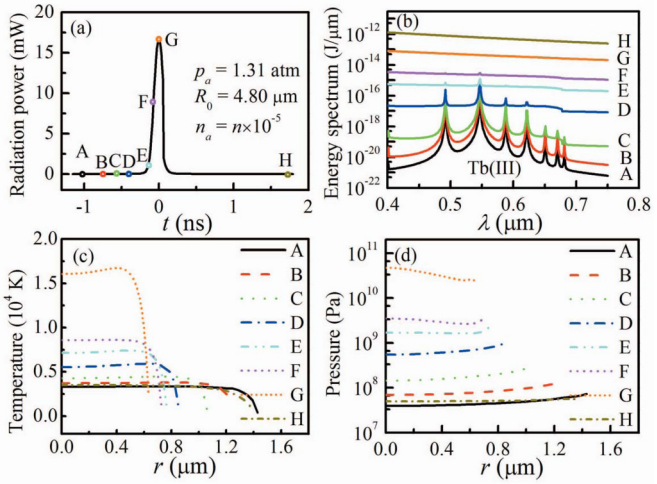

FIG. 4. Simulation results for an Ar bubble in a $Tb(NO_3)_3$ aqueous solution at 15 °C driven by an acoustical pressure of 1.31 atm [p_{a8} in Fig. 2(a)]. (a) Radiation power of the bubble versus time, (b) energy spectra, (c) temperature, and (d) pressure.

In Fig. 3, we obviously see that, when the temperature is relatively low (below about 9000 K), β of the theoretical calculation from Fig. 2(a) is greater than that of experimental data from Fig. 1, the reasons of which may be that: (1) the effect quenching the peak of the Tb(III) line by some species is ignored; (2) the transition rate of the Tb(III) ion may vary with temperature because of a collision between the Tb(III) ion and other particles, whereas it is as a constant in the present calculation simulation.

To further understand the process behind the appearance of the spectral lines, we simulate the light emission pulse from an Ar bubble in an aqueous solution of $Tb(NO_3)_3$ at 15 °C driven by an acoustical pressure of 1.31 atm [p_{a8} in Fig. 2(a)].

Figure 4(a) illustrates the total radiation power per flash of this simulated bubble, and we select eight moments (points

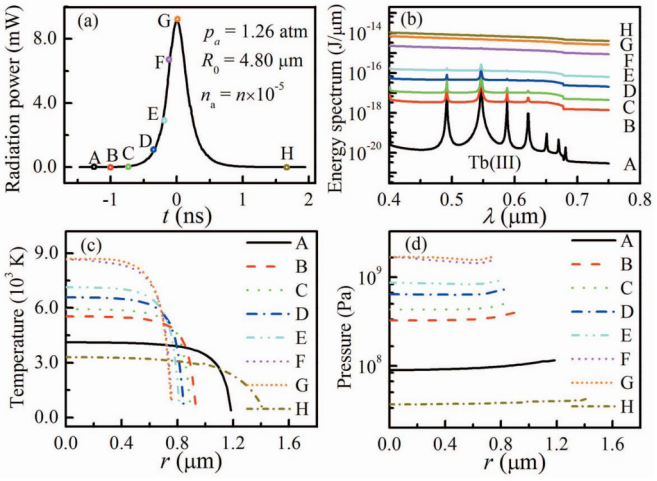

FIG. 5. Simulation results for an Ar bubble in a $Tb(NO_3)_3$ aqueous solution at 15 °C driven by an acoustic pressure of p_a = 1.26 atm [p_{a6} in Fig. 2(a)]. (a) Total radiation power versus time, (b) energy spectra, (c) temperature, and (d) pressure.

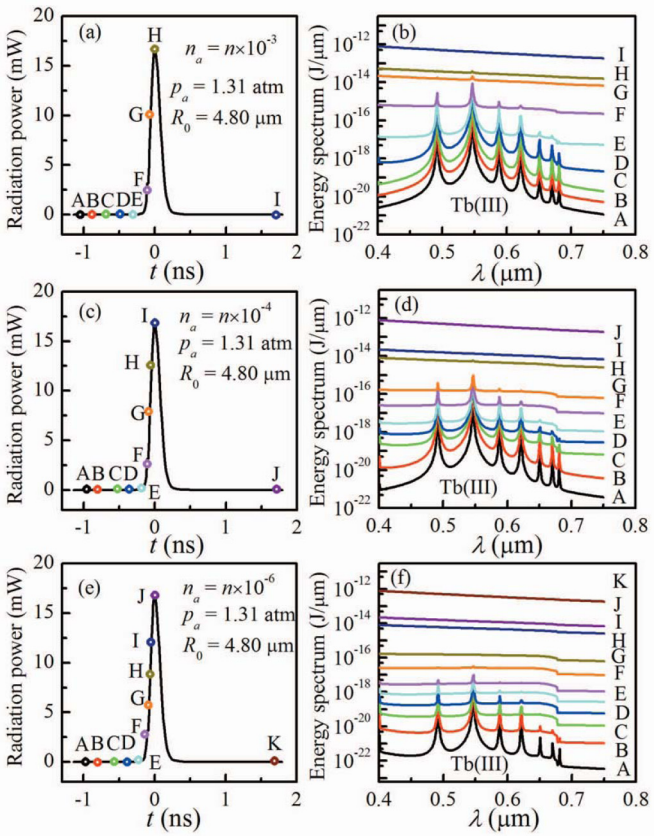

FIG. 6. Simulation results for an Ar bubble in a $Tb(NO_3)_3$ aqueous solution at 15 °C driven by an acoustic pressure of p_a = 1.31 atm. (a), (c), and (e) Total radiation power versus time. (b), (d), and (f) Energy spectra.

marked A–H) on the curve to evaluate the radiation energy spectrum [Fig. 4(b)] and the corresponding temperature and pressure [Figs. 4(c) and 4(d)] for moments before and after peak radiation. Since the radiation energy spectrum accumulates over time, the total intensity increases over each moment. As the radiation power increases from A to H [Fig. 4(a)], the intensity of the continuum background increases, and the Tb(III) spectral peaks in the region of 0.48–0.69 μm gradually disappear [Fig. 4(b)]. At the moment of maximum radiation (marked H), the bubble ceases to luminesce, and the corresponding energy spectrum equals that accumulated during one flash over one acoustic period.

As the simulated bubble collapses, the temperature obviously increases [Fig. 4(c)], and the temperature quickly decreases after the peak radiation occurs. The pressure distribution follows the same trend. Inside the bubble, the maximum temperature occurs at the center of the bubble during the whole cycle, and it drops off precipitously at the bubble wall. Pressure, on the other hand, is distributed evenly inside the bubble [Fig. 4(d)].

We simulate the light emission pulse and the energy spectra from an Ar bubble in an aqueous solution of $Tb(NO_3)_3$ at 15° for the case p_{a6} (p_a = 1.26 atm) as well as the corresponding temperature and pressure distributions in the bubble (see Fig. 5). The results follow similar trends as those for the case of p_{a8} (p_a = 1.31 atm).

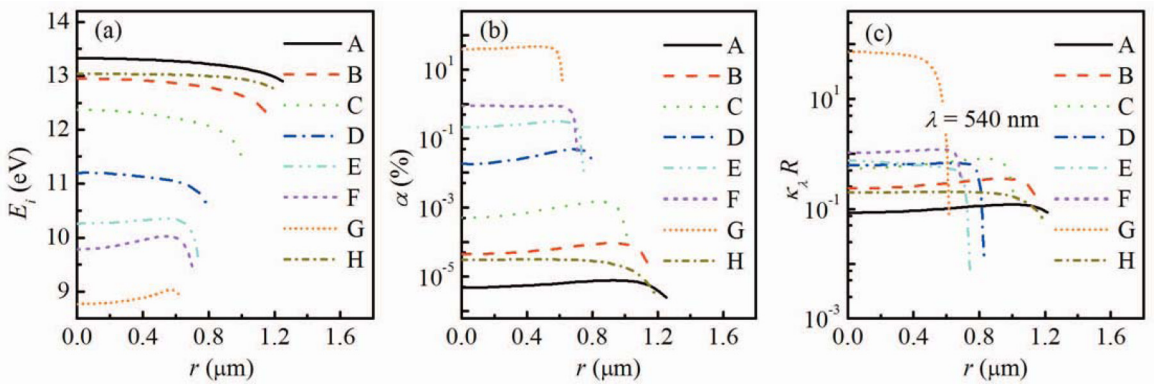

FIG. 7. Distributions of (a) E_i, (b) α, and (c) $\kappa_\lambda R$ at $\lambda = 540$ nm along the radius of a simulated bubble, corresponding to the moments (i.e., A,B, ...,H) marked in Fig. 4(a).

In our simulation, the number density (n_a) of Tb(III) is a parameter that is difficult to determine experimentally. To understand the effect of n_a on spectral intensity, we selected three cases ($n_a = n \times 10^{-3}$, $n \times 10^{-4}$, and $n \times 10^{-6}$, respectively, n is the total number density of particles inside a bubble) to simulate the process of spectral emission (see Fig. 6). Figure 6 shows that the intensity of Tb(III) line emission increases with n_a because the luminance of Tb(III) is proportional to its emitted photon number.

B. Ionization in the bubble

The ionization energy (E_i), the degree of ionization α, and the opacity in a SBSL bubble were determined in the present calculations using the methods reported in Refs. [21,22]. Figure 7 illustrates the temporal profile of the reduced ionization energy, the degree of ionization in an Ar bubble, and the opacities, the latter of which we determined by multiplying the absorption coefficient (κ_λ) with the bubble radius (R) [7]. These values correspond to the moments marked A–H in Fig. 4(a).

In Fig. 7(a) the reduced ionization energy of Ar atoms at the center of the bubble at time G is about 8.77 eV, which is greater than the first ionization energy of Tb(III) (about 2.5 eV). This represents a decrease of about 45% (the ionization energy of Ar is 15.8 eV). The reduced ionization energy indicates a degree of ionization of nearly 45% near the center of the bubble [Fig. 7(b)].

The results in Fig. 7(c) allow us to determine whether the simulated SBSL bubble would be transparent or opaque. For the transparent case of $\kappa_\lambda \lambda \ll 1$, spectral line emission may be observed, whereas for the opaque case of $\kappa_\lambda \lambda \gg 1$, these lines will be occluded from experimenters. For $\lambda =$ 540 nm, $\kappa_\lambda \lambda \ll 1$ at moments A, B, C, and H, so the bubble is transparent, and line emissions will appear (except at moment H because of the accumulated spectral radiation). For moments D and E, $\kappa_\lambda \lambda \approx 1$, so the bubble is translucent. For moments F and G, $\kappa_\lambda \lambda \gg 1$, so the bubble is opaque.

We also calculate E_i, α, and the opacity in a SBSL bubble for the p_{a6} case ($p_a = 1.26$ atm), which correspond to the moments marked A–H in Fig. 5(a). The calculated results follow similar trends as those for the p_{a8} case ($p_a = 1.31$ atm) (see Fig. 8).

IV. CONCLUSION

Our CFD simulation produced trends similar to previously observed line spectra emitted from Tb(III) within the sonoluminescing bubble of Ar gas. Therefore, our calculated distributions for temperature and pressure can be taken as reasonable models of the processes inside a sonoluminescing bubble. When the maximum temperature at the core of the bubble remains relatively low, simulated SBSL bubbles of

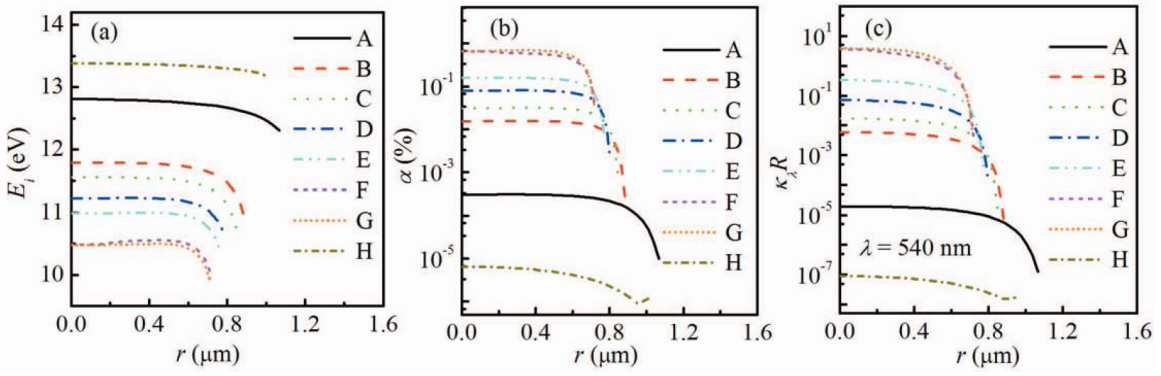

FIG. 8. Variations of (a) E_i, (b) α, and (c) $\kappa_\lambda R$ at $\lambda = 540$ nm with r inside a bubble, corresponding to the moments (i.e., A,B, ...,H) marked in Fig. 5(a).

the same size luminesce dimly, and spectral line emissions are prominent. As the maximum temperature increases, the spectral lines gradually are covered up by the continuum background. In other words, the spectral line emission dominates dim SBSL (usually at lower temperatures), whereas the continuum background dominates bright SBSL (usually at higher temperatures). Although both line emission intensities and continuum emission intensities increase with increasing temperature, continuum intensity increases more rapidly, which may explain the observed phenomena.

ACKNOWLEDGMENTS

The author J. Liang would like to thank Dr. W. Zhang for helpful discussions. This work was supported by the National Natural Science Foundation of China (Grants No. 11564006, No. 11334005, and No. 11574150), Guizhou Province Science and the Technology Innovation Talent Team [Grant No. (2015)4015] and the Key Laboratory of Low Dimensional Condensed Matter Physics of the Higher Educational Institution of Guizhou Province (Grant No. [2016]002).

[1] D. F. Gaitan, L. A. Crum, C. C. Church, and R. A. Roy, J. Acoust. Soc. Am. **91**, 3166 (1992).
[2] B. Gompf, R. Günther, G. Nick, R. Pecha, and W. Eisenmenger, Phys. Rev. Lett. **79**, 1405 (1997).
[3] S. Hilgenfeldt, S. Grossmann, and D. Lohse, Nature (London) **398**, 402 (1999).
[4] D. J. Flannigan and K. S. Suslick, Phys. Rev. Lett. **99**, 134301 (2007).
[5] Y. An, Phys. Rev. E **74**, 026304 (2006).
[6] Y. An and C. Li, Phys. Rev. E **78**, 046313 (2008).
[7] Y. An and C. Li, Phys. Rev. E **80**, 046320 (2009).
[8] T. J. Matula, R. A. Roy, P. D. Mourad, W. B. McNamara III, and K. S. Suslick, Phys. Rev. Lett. **75**, 2602 (1995).
[9] H. Xu, N. C. Eddingsaas, and K. S. Suslick, J. Am. Chem. Soc. **131**, 6060 (2009).
[10] C. Carlos, S. Julia, P. Rachel, and M. Robert, Ultrason. Sonochem. **21**, 2044 (2014).
[11] J. Xu, W. Chen, X. Xu, Y. Liang, W. Huang, and X. Gao, Phys. Rev. E **76**, 026308 (2007).
[12] V. Kamath, A. Prosperetti, and F. N. Egolfopoulos, J. Acoust. Soc. Am. **94**, 248 (1993).
[13] H. Yuan and A. Prosperetti, Phys. Fluids **9**, 127 (1997).
[14] G. L. Sharipov, B. M. Gareev, and A. M. Abdrakhmanov, JETP Lett. **91**, 566 (2010).
[15] R. Pflieger, S. Julia, S. Bertrand, M. Helmuth, and S. I. Nikitenko, J. Phys. Chem. B **117**, 2979 (2013).
[16] J. Liang, W. Chen, C. Zhou, W. Cui, and Z. Chen, Phys. Lett. A **379**, 497 (2015).
[17] F. S. Richardson, Chem. Rev. **82**, 541 (1982).
[18] J. B. Keller and M. Miksis, J. Acoust. Soc. Am. **68**, 628 (1980).
[19] R. Mavrodineanu and H. Boiteux, *Flame Spectroscopy* (Wiley, New York, 1965), pp. 41 and 382.
[20] Y. An and W. J. Zhang, Chin. Phys. B **21**, 17806 (2012).
[21] K. Yasui, Phys. Rev. E **64**, 016310 (2001).
[22] W. J. Zhang and Y. An, Chin. Phys. B **24**, 047802 (2015).
[23] T. Carrington, J. Chem. Phys. **30**, 1087 (1959).
[24] F. Grieser, J. Phys. Chem. **85**, 928 (1981).
[25] G. S. Ofelt, J. Chem. Phys. **38**, 2171 (1963).